Impact of conditions at start-up on thermovibrational convective flow

D. E. Melnikov, V. M. Shevtsova, and J. C. Legros*
Microgravity Research Center, Université Libre de Bruxelles, CP-165/62, Av. F.D. Roosevelt, 50, B-1050 Brussels, Belgium
(Received 14 May 2008; published 20 November 2008)

The development of thermovibrational convection in a cubic cell filled with high Prandtl number liquid (isopropanol) is studied. Direct nonlinear simulations are performed by solving three-dimensional Navier-Stokes equations in the Boussinesq approximation. The cell is subjected to high frequency periodic oscillations perpendicular to the applied temperature gradient under zero gravity. Two types of vibrations are imposed: either as a sine or cosine function of time. It is shown that the initial vibrational phase plays a significant role in the transient behavior of thermovibrational convective flow. Such knowledge is important to interpret correctly short-duration experimental results performed in microgravity, among which the most accessible are drop towers (~5 s) and parabolic flights (~20 s). It is obtained that under sine vibrations, the flow reaches steady state within less than one thermal time. Under cosine acceleration, this time is 2 times longer. For cosine excitations, the Nusselt number is approximately 10 times smaller in comparison with the sine case. Besides, in the case of cosine, the Nusselt number oscillates with double frequency. However, at the steady state, time-averaged and oscillatory characteristics of the flow are independent of the vibrational start-up. The only feature that always differs the two cases is the phase difference between the velocity, temperature, and accelerations. We have found that due to nonlinear response of the system to the imposed vibrations, the phase shift between velocity and temperature is never equal exactly to $\pi/2$, at least in weightlessness. Thus, heat transport always exists from the beginning of vibrations, although it might be weak.

DOI: 10.1103/PhysRevE.78.056306 PACS number(s): 47.20.Bp, 47.15.Rq, 47.55.pb

I. INTRODUCTION

Net convective heat and mass transfer exists in systems with spatially nonuniform density which are subjected to external vibrations. This phenomenon is attributed to the effect of inertia of the liquid and is more pronounced under microgravity. Convection is stronger when the density gradient and vibrations are perpendicular. The density gradient can be created by temperature inhomogeneity and, consequently, the phenomenon is called thermovibrational convection [1].

Thermovibrational convection is studied for decades. Russian school, e.g., [1–3] has developed an averaging approach to study the flows under high-frequency vibrations. Among the pioneer works should be mentioned the paper by Zenkovskaya and Simonenko [2], in which a method of averaging the Navier-Stokes equations was first successfully applied for studying the convective stability of the mechanical equilibrium of a horizontal fluid layer heated from below. In this approach, the physical quantities are considered as a superposition of slow (time-averaged) and rapid time-dependent contributions. It makes possible to obtain a closed system of differential equations for average velocity, temperature, and pressure fields.

Parameter, which defines stability boundary of the slow flow (also called mean flow), is the vibrational analogue of Rayleigh number, $\mathrm{Gs}=(A\Omega\beta_T L\Delta T)^2/(2\nu\alpha)$. We suggest to call it Gershuni number (instead of vibrational Rayleigh number) to mark a significant contribution of Gershuni to the theory of thermovibrational convection [1]. Here L, A, Ω are, respectively, the enclosure size, the displacement amplitude, and the frequency of vibrations; liquid properties β_T, ν, and α stand for the thermal expansion coefficient, kinematic viscosity, and thermal diffusivity; ΔT is the imposed temperature difference.

The advantage of this method of averaging is that one can obtain the final solution of the problem much faster than considering the full nonaveraged equations. But it is applicable only under some restrictions such as that the oscillation period to be much smaller than all the characteristic times, viscous $\tau_\nu=L^2/\nu$ and thermal $\tau_{th}=\tau_v\,\mathrm{Pr}$ (Prandtl number $\mathrm{Pr}=\nu/\alpha$), and that the displacement amplitude must be smaller than the size of the domain L. In most situations where these requirements are not met, an ordinary approach of solving the full Navier-Stokes equations must be utilized, which leads to much longer computations especially when tracking high frequency accelerations.

Gershuni and Lyubimov in [1] summarized numerous theoretical studies. The possibility of a mechanical quasiequilibrium state with zero mean flow (the oscillatory rapid component does not generally vanish) in a plane infinite fluid layer has been shown. It was obtained that in a layer the stability boundary is invariant regardless the value of Pr, while the steady mean flow can be different.

In a finite size system, the quasiequilibrium state is never possible. Even under very weak vibrations and small ΔT, a nonzero mean flow exists. Flow structure is defined by the Gershuni and Prandtl numbers. In a square cavity under 0-g a four-vortices structure sets in for the smallest Gershuni numbers. The critical Gs can be determined depending on thermal boundary conditions on lateral walls. This regime is stable for $\mathrm{Gs}<\mathrm{Gs}^{cr}$, and the motion undergoes a transition towards a single big diagonal vortex and a pair of corner vortices with opposite direction of circulation for $\mathrm{Gs}>\mathrm{Gs}^{cr}$.

In the case with gravity field, there are two convection excitation mechanisms, thermogravitational and thermovibrational. An inclined plane fluid layer in high frequency

*dmelniko@ulb.ac.be

vibrational and static gravitational fields was studied in [3]. Regions of convective stability of the quasiequilibrium state were determined by linear analysis for different orientations of gravity and vibrations. Somewhat similar problem was examined by Monti *et al.* [4], aimed at studying influence of g-jitter on convective flows on the space station. They have compared the direct numerical solution of the full Navier-Stokes equations with those, obtained by solving the time-averaged equations containing all of the g-jitter terms grouped in a single parameter. The problem was studied under the assumption of small amplitudes and large frequencies of the oscillatory g-jitter. Both approaches showed similar results. It was demonstrated that in the presence of both residual gravity and g-jitter a proper orientation of the experimental cell can be beneficial to reduce convective disturbances.

In the earlier days, the study of the effects of g-jitter on fluid flow was related to the crystal growth in space. A certain amount of studies have been done to estimate additional mass transport caused by vibrations. Alexander [5] has demonstrated that oscillatory flow can affect the mean transport of solute or dopant. Shevtsova *et al.* [6] have studied the effects of residual accelerations on behavior of a liquid phase by using three-dimensional modeling in a rectangular cavity with differentially heated walls. Very slow vibrations with a small amplitude were analyzed to meet the conditions encountered on-board spacecrafts. In a very wide range of the applied temperature difference (between 10 and 60 K), they found that as long as the accelerations oscillate around zero, the Nusselt number pulsates with double frequency of the g-jitter.

Gershuni *et al.* [7] performed a theoretical study on the stability of a plane horizontal layer of a binary mixture with Soret effect subject to static gravity and longitudinal high-frequency vibrations. Considering both positive and negative Soret effect, they analyzed contributions of different instability modes in destabilizing the system. Later, Zebib [8] has considered a double-diffusive system in a slot in a microgravity environment, and by means of two-dimensional linear stability analysis the effect of high frequency gravity modulation was investigated.

Recently, Shevtsova *et al.* [9] have reported results of a benchmark of numerical studies on the influence of slow vibrations on separation due to thermodiffusion in binary mixtures in a cubic enclosure. The impact of vibrations with different frequencies on the temperature and concentration fields was analyzed. They found that the heat and mass transport increased with the decrease of the imposed frequency. In the combined case of simultaneous static gravity and g-jitter, the nonlinear interaction of static and vibrational actions resulted in a larger amplitude of pulsations of the variables.

Laboratory experimental observations of the thermovibrational convection [10] are in good agreement with the theoretical predictions and thus justify the behavior of mean flows. However, until now, there is a lack of successful hydrodynamic experiments which systematically investigate the effects of vibrations on flows in a microgravity environment. The only known series of experimental studies were performed on board Mir space station using the ALICE-2 facility for supercritical fluids [11] and JUSTSAP experiment during the course of a Shuttle mission [12]. The study of thermovibrational convection in parabolic flights has been performed recently [13,14].

Presently the thermovibrational convection keeps on attracting scientific interest. There are several open problems related to this subject. One of them is how the accelerations at the start-up of the thermovibrational convection could influence the heat and mass transport. The effect of single frequency vibrations given as either sine or a cosine function ($\pi/2$ phase shifted) has received attention in a paper by Naumann [15]. He studied it in a horizontal long channel in weightlessness and indicated that the effect is highly dependent on the phase of the acceleration at the zero time moment. Cosine vibrations give virtually no transport and the average velocity is almost zero, while sine vibrations immediately create a strong net transport.

Nowadays, there are not many opportunities to perform long duration experiments under microgravity conditions. Most of the experiments in physical science are performed in drop towers (~5 s), parabolic flights (~20 s), and more rarely in sounding rockets (~400 s), and even much more seldom on satellites and ISS. To interpret correctly short-duration experimental results, one should take into account a lot of phenomena affecting the transient regime. The question about the influence of start-ups on the development of convection in the system under vibration has no obvious answer. Our particular interests to this transient regime and to the choice of parameters were motivated by microgravity experiments on the onset of thermovibrational convection performed during parabolic flights [13,14]. Even if 20 seconds of reduced gravity are enough to establish mean flow, it is too short for reaching the steady state. The present study is focused on the influence of the vibrations at start-up on three-dimensional thermovibrational flow in a cube under weightlessness in a transient regime.

II. FORMULATION OF THE PROBLEM

We analyze thermovibrational convection in a cubic cell filled with isopropanol (Pr=40) heated from above. Figure 1 shows the geometry of the problem and the adopted coordinates system. The cell is subjected to high frequency vibrations, i.e., when the period of vibration, τ_{os}, is much smaller than both viscous τ_ν and thermal τ_{th} characteristic times. The imposed external vibrations are perpendicular to the applied temperature gradient, and thus they cause the largest changes in the oscillatory flow field. The stationary gravity is absent, and single-frequency acceleration is time dependent with zero mean. If the cell's displacement is $x(t)=A\cos(2\pi ft+\phi)$, then the acceleration is

$$x''(t) = -A(2\pi f)^2 \cos(2\pi ft+\varphi)\mathbf{e} = -g_{os}F(t,\varphi)\mathbf{e}, \quad \text{where } g_{os}=A(2\pi f)^2, \qquad (1)$$

where $\mathbf{e}=(1,0,0)$ is the unit vector along the axis of vibration, A is the displacement amplitude in the x direction and f is the frequency. The phase ϕ is constant and defines the type of vibrations applied at the start-up. $F(t,\phi)=\cos(2\pi ft+\phi)$ can be either cosine or sine function.

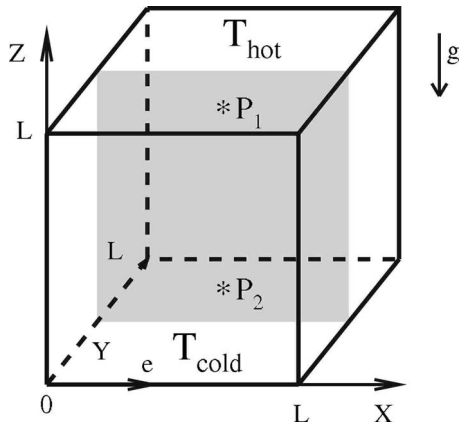

FIG. 1. Geometry and coordinate system. Points P_1 and P_2 show schematically the locations of data recordings versus time, and the gray vertical cross section is the plane where both temperature and velocity fields are visualized.

All the thermophysical properties of the liquid are constant, except the density ρ, which depends linearly on the local temperature T. The equation of state has the form

$$\rho(T) = \rho_0[1 - \beta_T(T - T_0)],$$

where T_0 is a reference temperature (we chose $T_0 = T_{\text{cold}} = 20\ ^\circ\text{C}$), $\rho_0 = \rho(T_0)$ and $\beta_T = -1/\rho_0 \partial\rho/\partial T > 0$ is the thermal expansion coefficient. The horizontal walls at $Z=0$ and $Z=L$ are kept at constant and uniform temperatures T_{cold} and T_{hot} ($T_{\text{hot}} > T_{\text{cold}}$), respectively. The vertical walls (at $X=0,L$ and $Y=0,L$) are thermally insulated. All the boundaries are assumed rigid, so nonslip conditions are valid for the liquid velocity $\mathbf{V}$.

The problem is governed by momentum, continuity, and energy equations

$$\frac{\partial \mathbf{v}}{\partial t} + \mathbf{v}\,\nabla\,\mathbf{v} = -\nabla p + \nabla^2 \mathbf{v} + \text{Gr}_{os} F(t,\varphi)\Theta \mathbf{e}, \tag{2}$$

$$\nabla \cdot \mathbf{v} = \mathbf{0}, \tag{3}$$

$$\frac{\partial \Theta}{\partial t} + \mathbf{v}\,\nabla\,\Theta = \frac{1}{\text{Pr}}\nabla^2 \Theta. \tag{4}$$

The following nondimensional variables were introduced:

$$x = X/L, \quad y = Y/L, \quad z = Z/L, \quad t = t'\nu/L^2, \quad \omega = 2\pi f L^2/\nu,$$

$$\mathbf{v} = \mathbf{V}L/\nu, \quad \Theta = (T - T_0)/\Delta T, \quad p = PL^2/\rho_0\nu^2,$$

here P is the pressure, t' is time, and $\Delta T = T_{\text{hot}} - T_{\text{cold}}$. The corresponding dimensionless boundary conditions are

$$\mathbf{v} = 0, \quad \Theta(z=0) = 0, \quad \Theta(z=1) = 1, \quad \mathbf{n}\cdot\nabla\Theta = 0,$$

$\mathbf{n}$ is the normal vector to the vertical walls $x=0,1$ and $y=0,1$.

At zero time moment, the liquid is motionless $\mathbf{v}(t=0)=\mathbf{0}$ and a linear temperature profile between the cold and the hot walls is established inside the cell $\Theta(t=0)=z$.

TABLE I. Phase φ and corresponding function $F(t,\varphi)=\cos(\omega t+\varphi)$.

φ	0	π	-0.5π	0.5π
F	$\cos(\omega t)$	$-\cos(\omega t)$	$\sin(\omega t)$	$-\sin(\omega t)$

The amplitude $A=7.5$ cm and $f=4$ Hz are chosen as these values of the parameters were used in experiments during parabolic flights [13,14]. The cell's size is $L=5\times10^{-3}$ m. The period of the oscillations is 37 times smaller than the viscous time ($\tau_v = L^2/\nu = 9.36$ s), and the amplitude is 15 greater than the size of the system L. Thus, at the chosen values, the averaging approach of governing Navier-Stokes equations is not valid and the problem is considered by solving the system of full nonlinear equations (1)–(4). The mean flow and temperature are calculated by averaging the appropriate variable over one oscillatory period,

$$\hat{\mathbf{v}}(t) = \frac{\omega}{2\pi}\int_t^{t+2\pi/\omega} \mathbf{v}(t')dt', \quad \hat{\Theta}(t) = \frac{\omega}{2\pi}\int_t^{t+2\pi/\omega} \Theta(t')dt'. \tag{5}$$

The problem is characterized by Prandtl, oscillatory Grashof numbers,

$$\text{Pr} = \nu/\alpha, \quad \text{Gr}_{os} = g_{os}\beta_T L^3 \Delta T/\nu^2,$$

and the vibrational function $F(t,\phi)$. The Gershuni number does not appear in such formulation of the problem, but it is related with Gr_{os} in the following way:

$$\text{Gs}/\text{Gr}_{os} = \text{Pr}\, A\beta_T \Delta T/2L.$$

Calculations are performed for $\Delta T = 7$ K. Thus, the oscillatory Grashof numbers and Prandtl number are fixed, Pr=40 and $\text{Gr}_{os}=6159$. The solution of the problem, Eqs. (2)–(4), is defined by the type of vibrational function $F(t,\phi)$. For the present study, we take four values of φ: 0, $\pi/2$, π, and $-\pi/2$, and their type is given in Table I.

III. NUMERICAL APPROACH

The governing equations (2)–(4) are discretized using the finite volume technique on a staggered grid where pressure and temperature nodes are placed at the center of control volumes, and the velocity components are positioned at the faces of these volumes. An equally spaced in each direction regular mesh $[32\times33\times32]$ covers the computational domain. Its uniformity allows second-order spatial accuracy of the solution.

Integration in time was done with an explicit single forward time step marching method. Computation of the velocity field at each time step is carried out with a projection method (see Chorin [16]). The main idea of the method is that the initial momentum equation may be splitted into two independent ones. As first, a "provisional" velocity field corresponding to the correct vorticity, but not satisfying the continuity equation (3), is computed neglecting the pressure gradient in the momentum equation. The equation defining the

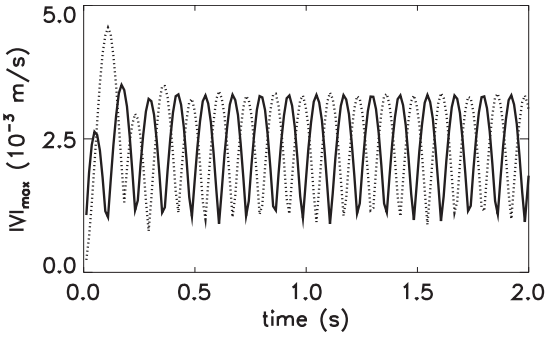

FIG. 2. Maximum absolute value of net liquid velocity within the first 2 seconds. Comparison between cosine (solid line) and sine (dotted line) start-ups.

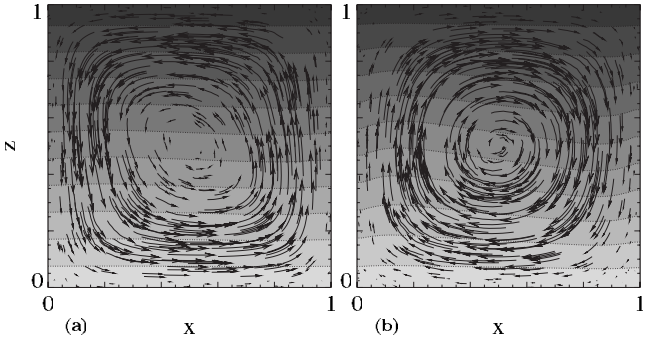

FIG. 3. Mean flows (arrows) and mean temperature fields (grey scale) in the vertical midplane of the cell after one period of oscillations (0.25 s). Vibrations are imposed as (a) $F=\cos(\omega t)$; (b) $F=\sin(\omega t)$.

velocity field on the next $n+1$ time level includes only the pressure gradient term.

Poisson equation for pressure is discretized using a combination of the fast Fourier transform (DFFT, 2^n+1 points) in the y direction and of an implicit alternating direction implicit (ADI) method at two other directions. The discretized Laplace equation for the pressure is solved by the iterative Thomas algorithm (see [17]). Finally, knowing the "provisional" velocity and the pressure, we advance in time getting the values of the velocity at the next time level from Eq. (2).

The CFD code used in this work has been tested and compared with other codes, which were independently developed by different research groups. Aiming at the codes validation, a double-diffusive convection in a binary mixture with negative Soret effect was benchmarked [9]. Three different groups have independently considered four problems by solving full three-dimensional Navier-Stokes equations. Good agreement of the results among the benchmark participants gave confidence to the developed CFD code.

IV. RESULTS AND DISCUSSION

A. Temporal evolution of mean flows

The phase of acceleration at $t=0$ plays a significant role in formation of the transient flow structure. Value of ϕ defines both duration and sign of the initial vibrational acceleration. If $F=\sin(\omega t)$, then during the first one-half of a period, vibrational forcing has the same sign ($F>0$). When $F=\cos(\omega t)$, it is positive during one-quarter of a period and is negative for the next one-half period, reversing the flow during this half-cycle. Thus, in the case of cosine the flow, which does not have enough time to get developed, should turn back after one-quarter of a period and its velocity diminishes. It means that $F=\sin(\omega t)$ produces much higher flow velocity after one oscillation period.

Figure 2 shows maximum absolute value of the flow $|V|_{\max}$ produced by $F=\cos(\omega t)$ (solid line) and $F=\sin(\omega t)$ (dotted line) vibrations. Calculations confirm that at the very beginning the flow velocity is larger when acceleration is a sine function: The first pick is the highest in the case of $F=\sin(\omega t)$ and the smallest under cosine vibrations. However, this additional mass transport at start-up in the sine case decays with time and the flow velocities become equal.

Consequently, structure of both the time-averaged (mean) flow $\hat{\mathbf{v}}$ and of the mean temperature $\hat{\Theta}$ [see Eq. (5) for their definition] depend on values of ϕ. The flow pattern $\hat{\mathbf{v}}$ observed in the cell after the first oscillation period is one big vortex (Fig. 3) both under $F=\cos(\omega t)$ and $F=\sin(\omega t)$ accelerations. Sine vibrations rotate vortex in a clockwise direction corresponding to initial positive acceleration [see Fig. 3(b), where the direction of the velocity vector is shown by arrows]. In the case of cosine, the direction of rotation remains clockwise only for one-half of a period, due to the positive value of $F(t,\phi)$ at $t=0$. Even though the vibrational acceleration was positive for the first one-quarter of a period, the first oscillation period finishes with a counterclockwise rotating vortex [Fig. 3(a)]. The fact that the average flow due to sine vibrations is much stronger could be seen in Fig. 3. The stronger flow produces stronger deformation of the temperature field (isotherms shown by grey scale). The latter stay almost straight when $F=\cos(\omega t)$.

The flow pattern with single large vortex exists only at the start-up and later in time the mean flow undergoes transition to the structure, shown in Fig. 4. Regardless the phase of imposed vibrations, the mean flow very quickly converges to the multiroll structure, which will be kept for a long time. The convergence takes a couple of vibrational periods.

Direction of the acceleration at the beginning is responsible for orientation of the convective flow. A difference between $\phi=0$ and π (the same is applied to $\phi=\pi/2$ and $-\pi/2$) is that $F(t,\phi)$ in Eq. (2) has opposite signs, and thus the convective roll gets different direction of rotation. It is easy to show that the flow $\mathbf{v}'$ and temperature Θ' resulted from $-F(t,\phi)$ are the ones obtained via solving the governing equations (2)–(4) with $F(t,\phi)$ after reversing the sign of the velocity in the direction of acceleration together with the appropriate transformation of coordinates,

$$v_x' = -v_x, \quad x' = 1 - x, \tag{6}$$

where $v_x=\mathbf{v}\cdot\mathbf{e}$. This is also valid for the time-averaged flow and temperature.

To check this, calculations were performed for four values of the phase ϕ (see Table I for the relations between values of the phase ϕ and type of vibrations). Figure 4 shows the time-averaged flows and temperatures at 20 s after the

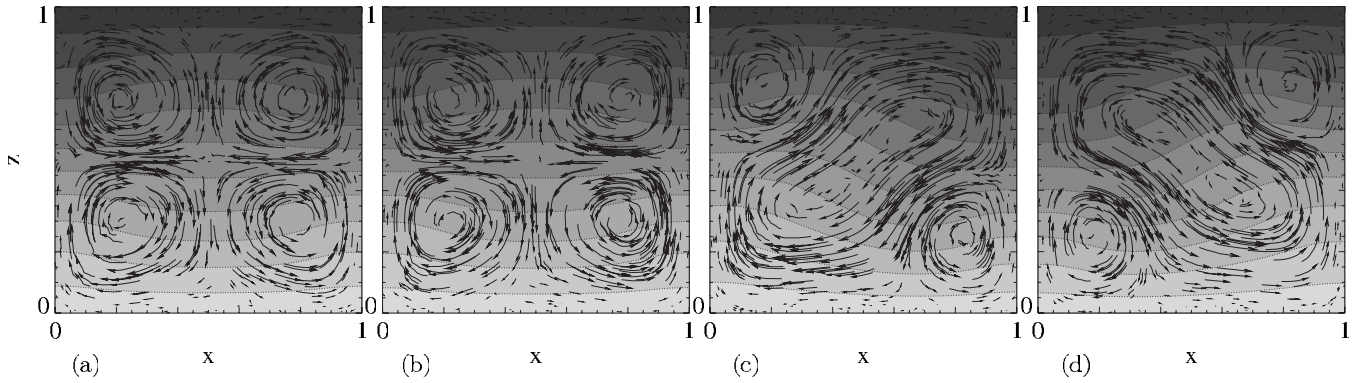

FIG. 4. Mean flows (arrows) and temperature fields (gray scale) in the vertical midplane of the cell at $t=20$ seconds. Vibrations are imposed as (a) $F=\cos(\omega t)$; (b) $F=-\cos(\omega t)$; (c) $F=\sin(\omega t)$; (d) $F=-\sin(\omega t)$.

start-up (approximately equal to two characteristic viscous times). Since this study was closely related to preparation of an experiment on thermovibrational convection under reduced gravity in parabolic flights, a 20-seconds interval is of particular interest because it is about the duration of a parabola trajectory producing a microgravity period. Usually vibrations start roughly at the beginning of the microgravity. The visualizations are done at the vertical midplane shown in grey in Fig. 1.

Figure 4 proves that the phase ϕ in Eq. (1) is a parameter responsible for the structure of the mean flow $\hat{\mathbf{v}}$ observed during a long time in the cell. Changing the direction of acceleration in one-quarter of a period results in a four-vortices mean flow [Figs. 4(a) and 4(b)]. Sine vibrations give the liquid an initial impulse of 2 times longer duration and, as a result, the average flow has a different structure [Figs. 4(c) and 4(d)].

The four-vortices flow is an intermediate regime passed by the system on its way to the final stable one-vortex flow shown in Figs. 5(c) and 5(d). Within one thermal time τ_{th} the four-vortices flow loses stability and becomes a single-vortex one [compare Figs. 4(a) and 5(a)]. The one-vortex flow, quickly established in the bulk in case of sine vibrations, is stable, and thus it does not change with time [see Figs. 4(c), 4(d), 5(c), and 5(d)].

Comparison between solutions at one thermal time with $\phi=0$ [Fig. 5(a)] and with $\phi=\pi$ [Fig. 5(b)] demonstrates that the mean flows are oppositely rotating and their directions are determined by the sign of $F(t,\phi)$ at the start-up. The solution in Fig. 5(b) is indeed the one with $\phi=0$ [Fig. 5(a)] transformed in accordance with Eq. (6). Note that the mean flow in Fig. 5(a) rotates in clockwise direction while after one oscillatory period it was oppositely oriented [see Fig. 3(a)].

In the framework of mean flows the Gershuni number Gs is used as a governing parameter. It follows from previous studies [1] that four-vortices mean flow regime is unstable when $\mathrm{Gs}>8000$ (in case of adiabatic lateral walls). The present calculations were performed for $\mathrm{Gs}=13\,705>\mathrm{Gs}^{cr}$, and although the solutions are obtained via solving the full three-dimensional Navier-Stokes equations, we clearly confirm that the four-vortices structure is time unstable. However, our results show that it is possible to generate the four-vortices mean unsteady flow during the transients via imposing appropriate vibrations with a correctly chosen phase ϕ.

Indeed, the four-vortices mean flow exists during a few viscous times and within one thermal time evolves towards the stable one-vortex structure. The exact lifetime of this regime will be analyzed below. It is interesting to compare our results with those by Naumann [15]. He obtained that, in the case of sine accelerations, the velocity oscillates around nonzero mean value while if the vibrations are a cosine function the mean flow is zero. The former is not confirmed by

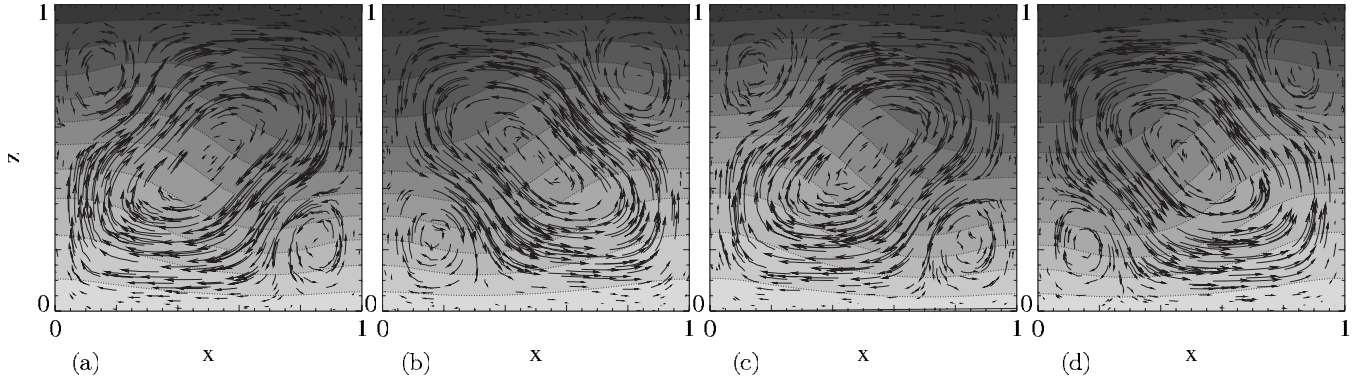

FIG. 5. Mean flows (arrows) and temperature fields (gray scale) in the vertical midplane of the cell at one thermal time (375 s). Vibrations are imposed as (a) $F=\cos(\omega t)$; (b) $F=-\cos(\omega t)$; (c) $F=\sin(\omega t)$; (d) $F=-\sin(\omega t)$.

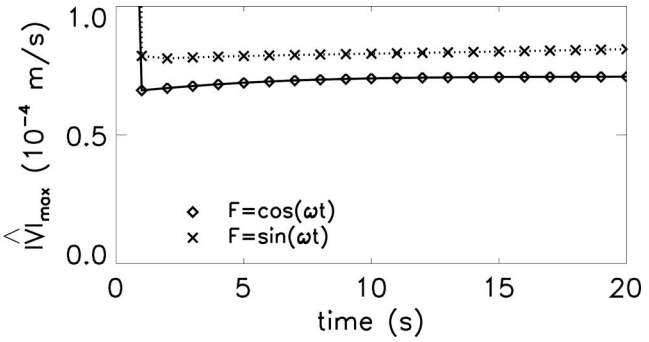

FIG. 6. Maximum absolute value of mean flow within the first 20 seconds. Comparison between cosine (solid line) and sine (dotted line) start ups.

the present results [see Figs. 4(a) and 6]. Obviously, the difference with [15] can be attributed to the variation in geometries and three dimensionality of the present problem. It was shown [1] that, even in a two-dimensional problem with finite aspect ratio, the presence of lateral walls in the direction of imposed vibrations always give a nonzero mean flow.

Maximal absolute values of the mean flow in the cell $|\hat{\mathbf{V}}|_{\max}$ for different initial phases are shown in Fig. 6. This function is time and coordinate dependent. In both cases the mean flows are nonzero and the maximal velocities of the mean flows have the same order of magnitude. Time-dependent evolution of $|\hat{\mathbf{V}}|_{\max}$ within the first 20 seconds is shown for $\phi=0$ (solid line) and $-\pi/2$ (dotted line). The mean flow reaches large values during the first vibrational period, $|\hat{\mathbf{V}}|_{\max}=0.42\times10^{-3}$ m/s and 1.52×10^{-3} m/s for cosine and sine, respectively (these values are out of the scaling in Fig. 6). They rapidly diminish to the end of the first second, as the flow pattern changes from one-roll to multiroll structure [compare Fig. 3 and Figs. 4(a) and 4(c)]. Although the values of $\hat{\mathbf{V}}$ at $t=0.25$ s are large, they are much less than the corresponding values of the full flow $\mathbf{V}=\hat{\mathbf{V}}+\mathbf{V}_{\mathbf{os}}$ (see Fig. 2 for comparison). The mean flow continuously grows, and the growth rate is slightly higher in the case of cosine accelerations.

B. Behavior of the oscillatory component of the flows

Although the value of $\hat{\mathbf{V}}$ is close to 10^{-4} m/s, which is very small, the velocity itself-oscillates with a much larger amplitude A_V [Fig. 7(a)]. Figure 7 shows time evolution of the amplitudes of velocity and temperature recorded near the hot boundary at the point $P_1=(0.45,0.5,0.83)$. Strongest growth of the velocity amplitudes occurs during the first vibrational period and then rapidly decreases in both cases. The peak values reach 3.5×10^{-3} m/s and 2.9×10^{-3} m/s for cosine and sine profiles, respectively. (There is no contradiction with Fig. 2 as here the quantities are analyzed at fixed point.) After initial 20 seconds (characteristic viscous time is $L^2/\nu_0=9.36$ s), the flow could be influenced only by the temperature field, the latter needs at least one thermal time $\tau_{th}=375$ to get stabilized. In the case of cosine acceleration A_V is always slightly larger (3.0 versus 2.93

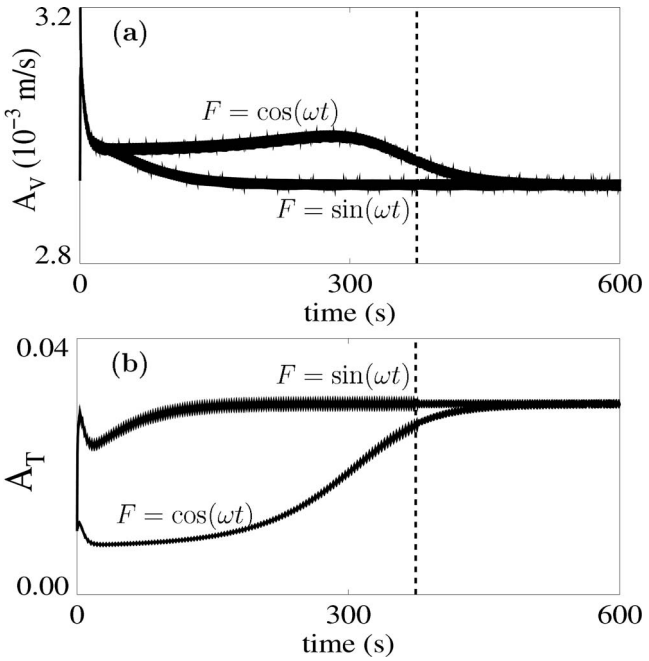

FIG. 7. Amplitude of velocity V_x (a) and of temperature (b) oscillations. Vertical dashed line shows one thermal time (375 s).

$\times10^{-3}$ m/s). Another difference in response of the system to the imposed vibrations is that when $F=\cos(\omega t)$ then for $t\leqslant300$ s, the velocity amplitude is growing and after $t\approx300$ s it diminishes approaching at the long time scale to the same value as in the case of sine acceleration. In the sine case, A_V is a monotonously decreasing function of time, and reaches stationary value at about one thermal time. To conclude, in the steady state the amplitude A_V of both vibrational functions have the same values regardless of the start-up.

Pulsations of the temperature field also depend on the start-up [Fig. 7(b)]. The difference with respect to the velocity oscillations is that the amplitude of temperature pulsations A_T is much larger in the case of sine acceleration. This difference is about a factor of 3, while A_V varies only by a small percentage of about 3%. The temperature is influenced by the thermovibrational convection but, due to the relatively large thermal time ($\tau_{th}\sim1500\tau_{os}$), response of the temperature to the vibrations is very weak. In both cases the amplitude of the temperature oscillations is very small with respect to the temperature scale, which is only 0.15% of ΔT. Similar to the velocity, in the case of sine vibrations A_T reaches its steady value much faster compared to cosine acceleration. Under sine vibrations, the amplitude of oscillations achieves steady state in roughly 2 times shorter time compared to the cosine vibration. The pulsations of the temperature (as of the velocity) become sustained at approximately 500 seconds (Fig. 7).

C. Analysis of phase differences

Hereafter, the phase difference between the velocity in the direction of vibration, V_x, temperature and driving force are examined. Results are summarized in Fig. 8 where they are shown versus time. The phase shifts were calculated by com-

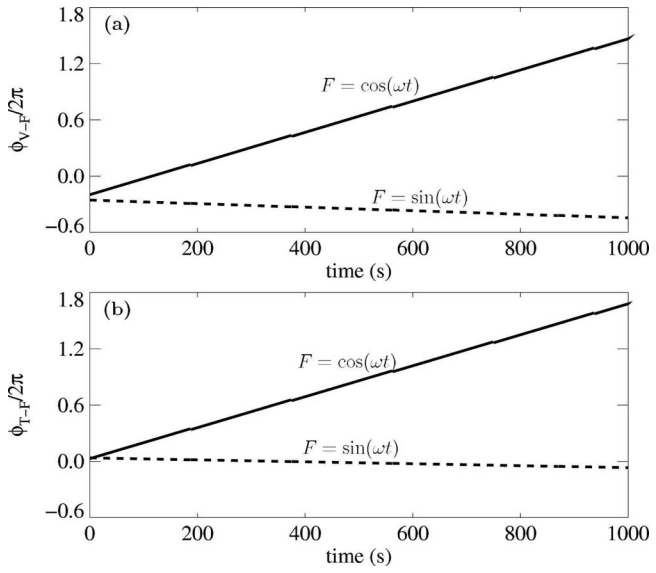

FIG. 8. Phase difference between velocity and acceleration φ_{V-F} (a) and between temperature and acceleration φ_{T-F} (b). Vertical dashed line shows one thermal time.

paring the consequent maxima of the corresponding time series. Negative value means that the maximum of acceleration occurred first. Analysis shows that the phase shift between velocity and imposed forcing, φ_{V-F}, behaves differently with time depending on ϕ. If the acceleration is a sine function, φ_{V-F} is very slowly changing with time:

$$\phi_{V-F} \approx -0.501\pi - 0.0003\pi t', \tag{7}$$

where t' is time in seconds. Its value is continuously decreasing by 0.11π within one thermal time. Even on a long time scale, this small additive is almost negligible.

But if the driving force is a cosine function, the phase lag between velocity and vibrations is growing 10 times faster [Fig. 8(a)] and again as a linear function of time,

$$\phi_{V-F} \approx -0.3958\pi + 0.00332\pi t'. \tag{8}$$

The solid line in Fig. 8 shows that at 20 s, the velocity and acceleration are almost out of phase, i.e., $\approx \pi/2$ (φ_{V-F} is normalized by 2π on the plot). At each thermal time, its value is growing at around 0.62π. Note that initial values of φ_{V-F} for sine and cosine are different.

In the case of cosine vibrations after one thermal time, i.e., $t=375$ s, the maximum V_x and maximum acceleration, F, are almost in the counterphase, meaning φ_{V-F} increases up to a close to π value. In the case of sine function, φ_{V-F} does not change with time as rapidly as in the case of cosine [compare Figs. 9(b) and 9(f)].

Behavior of the temperature pulsations repeats the one of the velocity with the only difference being the values at $t=0$ and slightly different growth rates. In the case of sine accelerations,

$$\phi_{T-F} \approx 0.0738\pi - 0.0002\pi t'. \tag{9}$$

When it is cosine,

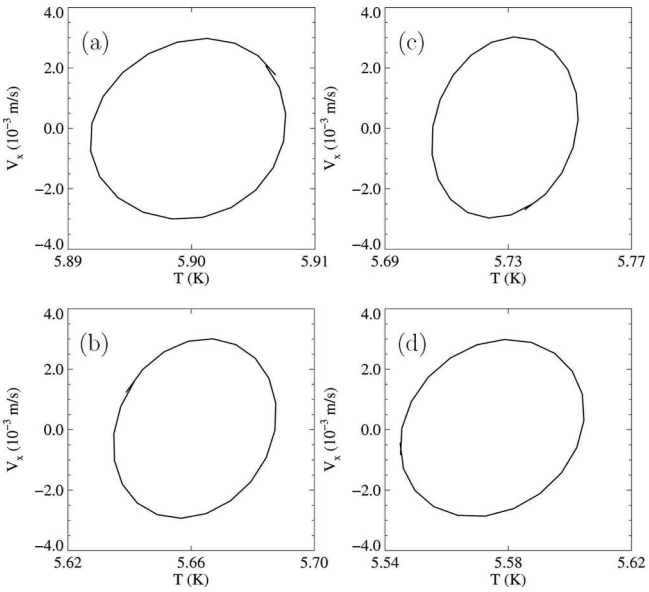

FIG. 9. Phase planes (velocity V_x versus temperature T) at 20 s and at one thermal time (375 s). Vibrations are imposed as $F=\cos(\omega t)$, (a) $t=20$ s, (b) $t=375$ s; $F=\sin(\omega t)$; (c) $t=20$ s, (d) $t=375$ s.

$$\phi_{T-F} \approx 0.0574\pi + 0.00330\pi t'. \tag{10}$$

The growth rates of the phase shifts between the variables and the accelerations are different: Negative in the case of sine vibrations and positive when the start-up is cosine function.

The analysis of the phases points out that the phase lags between V_x, T and external forcing are not constant in time. Because of the time-dependent lag, velocity and temperature oscillate with frequencies slightly different than the acceleration. The difference is subtle and the distinction is not usually noticed, but this effect accumulates and becomes important after a long time of integration. Let us consider a function (e.g., velocity) which oscillates with a frequency ω and has a time-dependent phase shift, $v \sim \cos[\omega t + \varphi(t)]$. Then the frequency of oscillations is equal to $(\omega + \partial\varphi/\partial t)/2\pi$, which gives an approximate value of 4.0016 Hz for the temperature and velocity pulsations in the case of cosine vibrations and leaving it almost unchanged at 4 Hz when $F=\sin(\omega t)$.

Let us examine the phase shift between velocity and temperature. In Fig. 9 we present the phase planes (V_x vs T) at different times and for different vibrational functions. The velocity and temperature are recorded near the hot boundary (at the point P_1). The plots are made at $t=20$ s and at one thermal time $t=\tau_{th}$ aiming at comparing the solutions for $F=\cos(\omega t)$ and $F=\sin(\omega t)$.

When driving force is cosine, the velocity-temperature phase shift is closer to 0.5π and trajectory on the phase plane is almost a cycle, see Fig. 9. Being approximately 0.4532π at $t=0$, it is linearly decreasing and after 1000 s is equal to 0.4332π. When the driving force is sine function, $\varphi_{V-T} \approx 0.5748\pi$, and after 1000 s it gets a larger value 0.6748π. According to estimations by Alexander in [5], the heat trans-

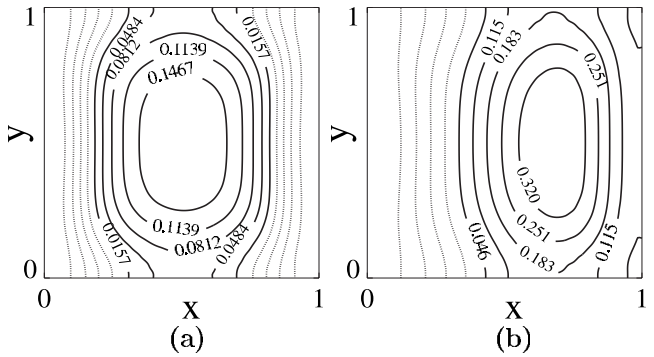

FIG. 10. Heat flux at the cold wall at $t=20$ s for different start-ups: (a) $F=\cos(\omega t)$, (b) $F=\sin(\omega t)$. Solid and dashed lines show, respectively, positive and negative heat flux q.

port (i.e., mean flow) does not arise when the phase shift between velocity and temperature is equal to $\pi/2$. On the other side, in the frame-of-averaging approach developed by Gershuni and Lyubimov [1] the mean flow always exists in the finite system in weightlessness for arbitrary small vibrations. Our time-dependent calculations resolve this contradiction: due to nonlinear response of the system on imposed vibrations, the phase shift between velocity and temperature φ_{V-T} is never equal to $\pi/2$. For cosine vibrations it is smaller than $\pi/2$, being a decreasing function, and the maximal value over time is $\varphi_{V-T}=0.45<\pi/2$. For sine function the phase shift is larger than $\pi/2$, being a slowly growing function, and the minimal value over time is $\varphi_{V-T}\approx 0.58$.

Following the idea that mean flow does not exist when $\varphi_{V-T}=\pi/2$, one may assume that the heat transport (mean flow) should be weaker when the system is in the vicinity of this point. However, the examination of the heat transport via Nusselt number does not support this idea.

D. Heat transfer by vibrations

Due to the imposed vibrations, the temperature field oscillates everywhere in the bulk and its time mean value deviates from the initially linear profile. The structure of the temperature field is defined by the mean flow $\hat{\mathbf{V}}$, which is slowly varying with time. The four-vortices symmetric flow [see Figs. 4(a) and 4(b)] shifts the isotherms in the central part of the cell towards the horizontal walls increasing the heat transfer at the middle of these walls. The dimensionless convective heat flux $q=(d\theta/dz-1)$ near the cold wall is shown in Fig. 10(a) at $t=20$ s. Indeed, at the central part heat flux achieves its maximal value. At the same time, moving away from the center (at x direction) the flow transports the colder liquid, decreasing the heat flux, and finally on the half-way to the lateral walls it becomes negative. Since the four vortices are almost symmetrical, the net convective heat transfer is weak. In the case of $F=\sin(\omega t)$, the powerful diagonal vortex generates stronger flow and the deviation of the isotherms from linear profile is larger, see Figs. 4(c) and 4(d). In addition, this flow is not symmetrical and, consequently, the maximum of heat flux is achieved closer to the right-hand lateral wall, see Fig. 10(b). Relatively weak negative flux is caused by the small corner vortex with the opposite direction of circulation. Thus, in the latter case the net heat flux will be larger.

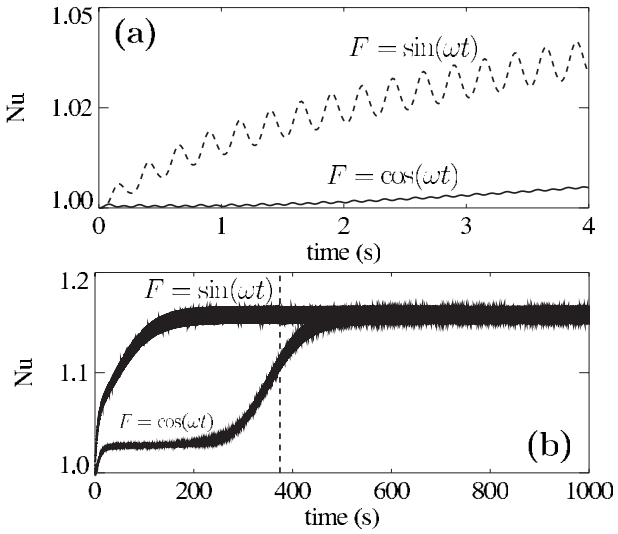

FIG. 11. Time evolution of Nusselt number on the cold wall. Vertical dashed line shows one thermal time.

To describe the integral heat transfer (conductive and convective) the Nusselt number, Nu, is introduced as

$$\mathrm{Nu}=\int \frac{d\Theta}{dz}(z=0)dxdy. \tag{11}$$

Figure 11 shows time evolution of the Nusselt number on the cold boundary. Starting with a sine function of acceleration causes significant increase in initial transport. This is not the case if the acceleration is a cosine function. Evolution of the heat transport during the first one-half of viscous time is shown in Fig. 11(a). Our results for the transient regime are in good agreement with those by Naumann [15], who plotted $\mathrm{Nu}(t)$ during one-half of the viscous time, which was $\tau_\nu/2\approx 300$ s. When $t=\tau_\nu/2$ the convective heat transfer in the case of the cosine function is one order of magnitude smaller than for the sine function.

Besides, in the case of cosine, the Nusselt number oscillates with double frequency [see Fig. 12(b)]. This frequency doubling of oscillations of Nu has been observed earlier in [6] where a three-dimensional thermovibrational convection in a rectangular cell was studied. An influence of a very slow g-jitter of a frequency 1.67×10^{-3} Hz on a fluid flow was studied in the case of lateral heating. In the case when steady component of gravity g_{st} in the direction of vibrations was absent, the Nusselt number oscillated with a double frequency because such vibrations should produce a four-vortices mean flow. It was shown that in the presence of an even very small g_{st}, Nu oscillated with the frequency of the external vibrations.

It can be explained in the following way. Velocity of the four-vortices flow is small meaning that the terms $\mathbf{v}\nabla\mathbf{v}$, $\mathbf{v}\nabla\Theta$ in Eqs. (2)–(4) can be neglected, and the governing equations can be linearized. The response temperature to the external perturbation does not have pure sinusoidal form and contains a whole spectrum of harmonics $\Theta\sim\theta_m e^{\pm im\omega t}$, e.g.,

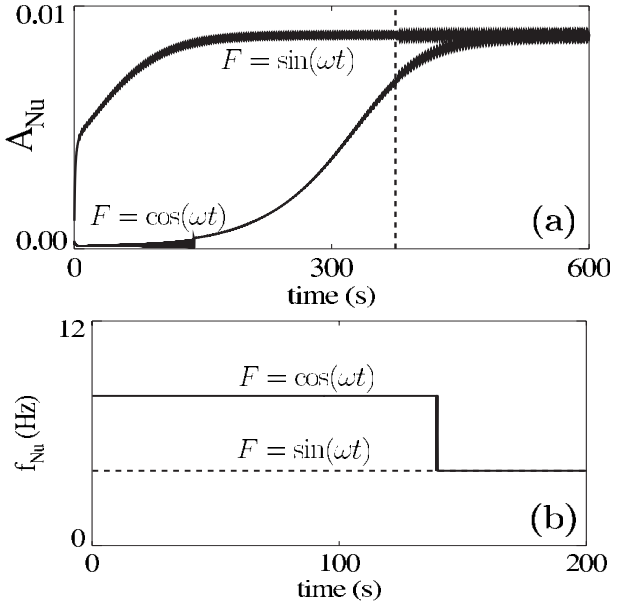

FIG. 12. Amplitude (a) and frequency (b) of oscillations of Nusselt number [Eq. (11)] on the cold wall. Vertical dashed line shows one thermal time.

$\theta_1 \cos(\omega t) + \theta_2 \cos(2\omega t) + \ldots$. This nonlinear component of the flow and temperature fields are symmetrical with respect to the cell center, but of opposite signs; look at Fig. 10(a) where temperature deviates in the opposite directions from the linear profile at the left- and right-hand parts. As the Nusselt number is an integral value, input from the different components with the main frequency [$\sim\cos(\omega t)$] is annihilated. The first super harmonics will in turn provide the input to the Nusselt number. Since the amplitude of the first harmonic is much smaller than the amplitude of the main frequency, deviation of the Nu number from unity due to the convective heat transport is approximately one order of magnitude smaller with respect to the sine case. Correspondingly, Nu oscillates with a frequency of 2ω.

In the case of $F=\sin(\omega t)$ the velocity is still small and the same expansion will be valid. But the components with the main frequency will not result in zero input as the flow is not symmetrical, see Fig. 10(b).

Despite the small value, the heat transfer in the four-vortex transient regime is increasing approximately during the time until this regime develops $t \leqslant 2\tau_\nu$. The growth rate of the Nusselt number decelerates during the next transition, when the one-vortex stable regime bifurcates from four-vortices to one, see Fig. 11(b). During this transition, the vibrational part of the flow also gets modified. The amplitude of the Nusselt number and its frequency are shown in Fig. 12. Until $t=140$ s it oscillates with a double frequency and with a negligible amplitude. Perhaps at $t=140$ s the recently appeared one-vortex flow becomes strong enough to turn the frequency to the value, equal to the frequency of the external forcing. Later in time, the heat transfer (i.e., mean temperature field) rapidly increases and reaches the same value as for the sine start-up. Besides, the oscillatory part of the flow starts to behave similar to the case of the sine acceleration. Inherently, the amplitude of Nu and the one of the temperature behave very similar in both cases [compare Figs. 7(b) and 12(a)]. Interestingly, in the case of the cosine accelerations after one thermal time, the temperature field still did not approach its steady final state.

If the acceleration is a sine function, the one large vortex flow gradually increases intensity with time, reaching the steady state within an interval shorter than thermal time. Consequently, the Nusselt number has stronger growth rate, and from the very beginning it oscillates with a large amplitude and with a frequency of the imposed vibrations [upper dotted line in Fig. 11(a)].

V. CONCLUSIONS

The effect of vibrational accelerations on the behavior of a liquid with Pr=40 in a cubic cavity with differentially heated horizontal walls have been studied using three-dimensional modeling. The phase of vibrational impact at the start-up plays a significant role in the development of thermovibrational convection. The temporal dynamics of the system at the initial stage are investigated when the acceleration is represented by a sine or a cosine function. The structure of time-averaged (mean) fields was examined on a long time scale, i.e., during a few thermal times. For vibrational stimuli $F=\cos(\omega t)$, the following sequence of mean flow regimes have been observed: One big central vortex with counterclockwise direction of circulation ($t \leqslant 0.25$ s) $\Rightarrow$ four-vortex regime $\Rightarrow$ one big diagonal vortex with clockwise direction of circulation and two small corner vortices. For vibrational stimuli $F=\sin(\omega t)$, the mean flow dynamics is different: one big central vortex with clockwise direction of circulation ($t \leqslant 0.25$ s) $\Rightarrow$ one big diagonal vortex with clockwise direction of circulation and two small corner vortices. The existence of the four-vortices intermediate regime in the cosine case affects local and integral characteristics, such as temperature and velocity pulsations, Nusselt number and time lags between physical quantities. However, after two thermal times the system approaches the same final steady state regardless of the start-up.

Starting with sine accelerations causes significantly larger initial transport, than if the accelerations start as a cosine function. Four-vortices structure existing under cosine vibrations produces very weak mean flow and, correspondingly, weak heat transfer. Besides, in this case, the Nusselt number on the cold and hot walls oscillates with double frequency. One may find an explanation of this behavior in Sec. IV D of the paper. Transition from four-vortex structure to one big diagonal roll occurs rapidly; after that the heat transfer is quickly increased and reaches the same value as for sine start-up.

The transient behavior of oscillatory parts of the flow is rather curious. In both cases the amplitude of temperature oscillations is tiny with respect to its characteristic value. Velocity amplitude has the same order of magnitude (or larger) as the mean flow. Moreover, the amplitude of velocity oscillations is larger for cosine acceleration while amplitude of temperature oscillations is larger for sine acceleration.

Phase shift between velocity and temperature and/or concentration has been examined by several authors when peri-

odic oscillations are normal to the density gradient [6,15,5]. Alexander [5] has evaluated that the heat-mass transport (i.e., mean flow) does not arise when the phase shift between velocity and temperature is equal to $\pi/2$. On the other hand, the averaging approach developed by Gershuni and Lyubimov [1] always predicts a nonzero mean flow in a finite system in weightlessness. Our time-dependent calculations resolve this contradiction: due to nonlinear response of the system on the imposed vibrations, the phase shift between velocity and temperature φ_{V-T} is never equal to $\pi/2$, at least in weightlessness. For cosine vibrations, it is smaller than $\pi/2$, being a decreasing function, and its maximal value over time is $\varphi_{V-T}=0.45\pi<\pi/2$. For sine function, the phase shift is larger than $\pi/2$, being a slowly growing function and its minimal value over time is $\varphi_{V-T}\approx 0.58\pi$.

ACKNOWLEDGMENTS

This work is supported by the PRODEX Programme managed by the European Space Agency in collaboration with the Belgian Federal Science Policy Office.

[1] G. Z. Gershuni and D. V. Lyubimov, *Thermal Vibration Convection* (Wiley, West Sussex, England, 1998).
[2] S. M. Zenkovskaya and I. B. Simonenko, Izv. Akad. Nauk SSSR, Mekh. Zhidk. Gaza **5**, 51 (1966).
[3] V. A. Demin, G. Z. Gershuni, and I. V. Verkholantsev, Int. J. Heat Mass Transfer **39**, 1979 (1996).
[4] R. Monti, R. Savino, and M. Lappa, Acta Astronaut. **48**, 603 (2001).
[5] J. I. D. Alexander, Microgravity Sci. Technol. **7**, 131 (1994).
[6] V. M. Shevtsova, D. E. Melnikov, and J. C. Legros, Microgravity Sci. Technol. **15**, 49 (2004).
[7] G. Z. Gershuni, A. K. Kolesnikov, J. C. Legros, and B. I. Myznikova, J. Fluid Mech. **330**, 251 (1997).
[8] A. Zebib, Phys. Fluids **13**, 1829 (2001).
[9] V. Shevtsova, D. Melnikov, J. C. Legros, Y. Yan, Z. Saghir, T. Lyubimova, G. Sedelnikov, and B. Roux, Phys. Fluids **19**, 017111 (2007).
[10] M. P. Zavarykin, S. V. Zorin, and G. F. Putin, Dokl. Akad. Nauk SSSR **299**, 309 (1988).
[11] Y. Garrabos, D. Beysens, C. Lecoutre, A. Dejoan, V. Polezhaev, and V. Emelianov, Phys. Rev. E **75**, 056317 (2007).
[12] J. Naumann, G. Haulenbeek, H. Kawamura, and K. Matsunaga, Microgravity Sci. Technol. **13**, 22 (2001).
[13] D. E. Melnikov, I. I. Ryzhkov, A. Mialdun, and V. Shevtsova, Microgravity Sci. Technol. **20**, 29 (2008).
[14] A. Mialdun, I. I. Ryzhkov, D. E. Melnikov, and V. Shevtsova, Phys. Rev. Lett. **101**, 084501 (2008).
[15] R. J. Naumann, Int. J. Heat Mass Transfer **43**, 2917 (2000).
[16] A. J. Chorin, Math. Comput. **22**, 745 (1968).
[17] L. H. Thomas, Watson Scientific Computer Laboratory Report, 1949 (unpublished).